

Journal Pre-proof

Characterisation of Electrospun PS/PU Polymer Blend Fibre Mat for Oil Sorption

Muftau J. Akanbi, Suwan N. Jayasinghe, Adam Wojcik



PII: S0032-3861(20)30954-X

DOI: <https://doi.org/10.1016/j.polymer.2020.123129>

Reference: JPOL 123129

To appear in: *Polymer*

Received Date: 2 July 2020

Revised Date: 6 October 2020

Accepted Date: 8 October 2020

Please cite this article as: Akanbi MJ, Jayasinghe SN, Wojcik A, Characterisation of Electrospun PS/PU Polymer Blend Fibre Mat for Oil Sorption, *Polymer*, <https://doi.org/10.1016/j.polymer.2020.123129>.

This is a PDF file of an article that has undergone enhancements after acceptance, such as the addition of a cover page and metadata, and formatting for readability, but it is not yet the definitive version of record. This version will undergo additional copyediting, typesetting and review before it is published in its final form, but we are providing this version to give early visibility of the article. Please note that, during the production process, errors may be discovered which could affect the content, and all legal disclaimers that apply to the journal pertain.

© 2020 Published by Elsevier Ltd.

CRedit

Muftau J. Akanbi: Conceptualization, Methodology, Investigation, Writing – original draft.

Suwan N. Jayasinghe: Supervision, Project administration, Resources.

Adam Wojcik: Writing – review & editing, Supervision, Validation, Resources

Journal Pre-proof

Abstract

Electrospun polystyrene (PS) fibre mat has been shown to have great potential as an oil sorbent due to its high sorption capacity and oil-water selectivity. Poor mechanical properties, due to the lack of inter-fibre bonding, has been a limiting factor in its use in such applications. In this study, mats of polymer blends of polystyrene (PS) and thermoplastic polyurethane (PU) fibres, in different polymer weight ratios, were produced and investigated for possible oil sorption application.

A comprehensive physico-chemical, thermal, mechanical and sorption characterisation of the different polymer blends was undertaken, to examine the effect of blend ratio on the fibre mat. Characterisation was by field emission scanning electron microscopy (FESEM), energy dispersive x-ray (EDX) spectroscopy, attenuated total reflectance fourier transform infrared (ATR-FTIR) spectroscopy, differential scanning calorimetry (DSC), thermo-gravimetric and differential analysis (TG-DTA), mechanical tensile testing, and by sorption analysis.

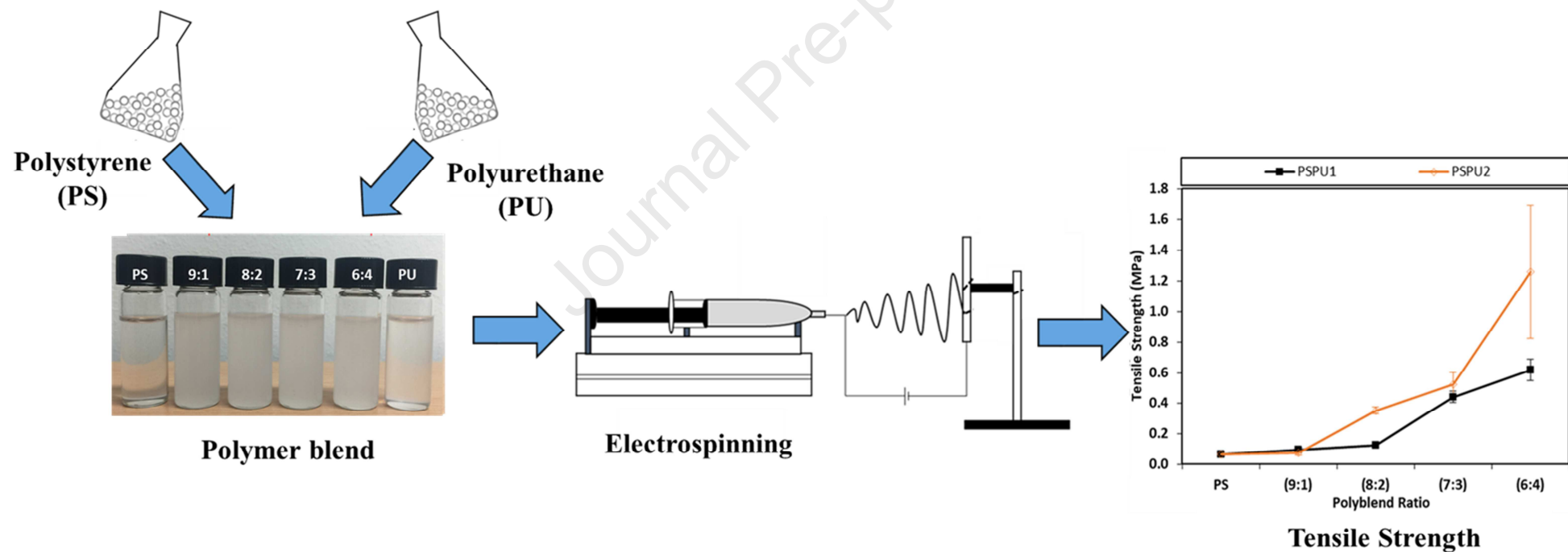
The microstructural properties of the fibres appeared significantly dependent upon the relative blend ratio. DSC revealed that good interaction/miscibility existed between the two polymers. Tensile strength characterisation showed that a pure PS fibre mat had a poor tensile strength, but the value increased over one order of magnitude with the addition of PU in the polymer matrix, attributed to the formation of inter-fibre bonds. Conversely, the sorption capacity (SC) decreased with increasing PU addition. Modulating the blend ratio could therefore provide a balance between the desired sorption capacity and the mechanical behaviour of resultant mats.

Sorption capacity is a complex interaction between fibre and mat characteristics but the polymer blend technique reported here offers a simple, effective and inexpensive method of addressing the poor mechanical properties of electrospun PS fibre, through enhancing micro/nano scale interactions between the two polymers in the blend.

Graphical Abstract

Characterisation of Electrospun PS/PU Polymer Blend Fibre Mat for Oil Sorption

Muftau J. Akanbi, Suwan N. Jayasinghe and Adam Wojcik

Correspondence to: Adam Wojcik (Email: a.wojcik@ucl.ac.uk)

Characterisation of Electrospun PS/PU Polymer Blend Fibre Mats for Oil Sorption

Muftau J. Akanbi, Suwan N. Jayasinghe and Adam Wojcik

Department of Mechanical Engineering

University College London

Torrington Place, London.

WC1E 7JE

Correspondence to: Adam Wojcik (Email: a.wojcik@ucl.ac.uk)

Keywords:

Electrospinning, Polymer Blend, Thermal Properties, Mechanical Characterisation, Oil Sorption, Oil Spillage Remediation

Journal Pre-proof

1. Introduction

Activities associated with oil exploration, production, transportation and storage pose significant risk of spillage and environmental damage[1, 2]. Oil spills can occur on either land or at sea, but spills over water often generate the greatest, environmental impact, damaging marine ecosystems for years or even decades[3]. A spill over water is not only a loss of a vital energy resource but a devastating blow to aquatic habitats, often times leading to the death of substantial quantities of sea life, as exemplified by events such as the Exxon Valdez Oil Spill of 1989, and the British Petroleum Deepwater Horizon (DWH) disaster of 2010[1, 4] and more recently the MV Wakashio oil spill off the coast of Mauritius in July 2020.

Several methods exist for oil spill remediation, such as the use of dispersants, in-situ burning, use of sorbents, and the deployment of skimmers[5]. These methods are often used in combination, as no single method best covers all situations. Amongst these, the use of sorbents is considered a very effective and economical method for oil spill remediation on both land [6] and on water. In effect, the use of sorbents facilitates the transformation of oil from a liquid to a semi solid state making the removal and subsequent recovery of the oil possible[7, 8]. It has also been identified as an effective way of mopping up polycyclic aromatic hydrocarbons (PAHs) from water[9], which often are an accompanying problem in oil spill situations. PAHs have been classified by the International Agency for Research on Cancer (IARC) and European Commission EC 2000 as priority pollutants, due to their high carcinogenic and mutagenic effect upon humans[10], and they often constitute a substantial part of crude oil[9].

Sorbents used in oil spill remediation can be classified into; inorganic mineral sorbents, organic natural sorbents and synthetic organic sorbents[1, 4, 8, 11, 12]. In the case of oil

spills at sea, the use of inorganic minerals is less common due to their low sorption capacity[5] and inadequate/poor buoyancy. Similarly, organic natural sorbents have a low sorption capacity and poor oil water selectivity[13, 14], so again are not widely employed. Meltblown polypropylene is the commercially available material widely used as oil sorbent but it exhibits low sorption capacity and poor oil-water selectivity[12, 14].

In a bid to develop a mat based material with better sorption performance, electrospinning (ES), a technology capable of producing fibres with diameter in the nano/micro-meter range, has been used to produce polystyrene and/or polystyrene-based mat[12, 14]. The choice of polystyrene hinges on the low surface energy of the bulk polymer, as well as its ability to be electrospun from a solution. Studies have shown that these materials have a better oil sorption capacity and oil water selectivity [14, 15] than commercial meltblown polypropylene (PP) sorbent. Unfortunately, poor mechanical strength makes handling a challenge particularly after sorption has occurred. The reason for the poor strength is not fully understood but it is probably due to an absence of physical interlinking between fibres, hence permitting interfibre movement and collapse under load.

Coaxial needle[16] and multi-nozzle[17] side-by-side electrospinning of PS and polyurethane (PU) have been used to address the issue of poor mechanical strength. These methods, however, use complex and expensive nozzle configurations and importantly do not guarantee a nano-level integration of the two polymers[18–20], which could be an important factor in generating optimum mechanical properties.

In this study, a polymer blend of PS and an ether based (thermoplastic) polyurethane (PU), was fabricated into fibre mats using a conventional single nozzle electrospinning approach. The rationale here was to create a far more intimately blended, (and hence isotropic), polymer fibre whose formulation could be varied experimentally, whilst also characterising properties

and thereby shedding light on the mechanism by which PU appears to strengthen PS based mats. This is in contrast to previous studies, where co-axial or multi-nozzle side-by-side spinning (rather than blend spinning) was used as a means of “incorporating” the PU. To this end, PSPU fibre mats of different PS/PU weight ratios were fabricated and a detailed morphological, thermal, mechanical, and sorption characterisation study was performed.

2. Materials and Methods

2.1 Electrospinning (ES)

Solution electrospinning requires all polymers to be dissolved in an appropriate carrier solvent. This is then delivered to a spray head via a syringe pump. The head is energized by a high voltage (HV) supply and liquid emerges from the nozzle as a jet. It is both drawn and thinned out by the action of the voltage, and solidifies by evaporation of solvent.

Polystyrene (PS) polymer of $M_w \sim 350,000$ g/mol, ACS grade solvents; N`N dimethylformamide (DMF) and tetrahydrofuran (THF) (Sigma Aldrich, UK) and two thermoplastic polyurethanes (TPU); pellethane 2363-80AE (PU1) and pellethane 5863-82AE (PU2) (kindly provided by Lubrizol Advanced Materials, Germany) were employed in this study. All polymers and solvents were used as supplied, without further purification. The physical characteristics of the different oils used for the determination of sorption behaviour are as shown in table 1.

Table 1: Physical properties of the oils used in this study

Oil Sample	Viscosity (mPas)	Density (g/cm³)
Light Crude Oil	0.13	0.794
Vegetable Oil	28	0.861
Sunflower Oil	37	0.894
Motor Oil 1	95	0.812

In conventional electrospinning, a mixture of solvents is often employed in order to obtain fibres of desired morphological structure[21]. The solvent mix ratio used in this study was determined from a preliminary experimental study by dissolving PS (20% w/w conc.) in different DMF/THF mixtures of weight ratios: 5:0; 4:1; 3:2; 2:3; 1:4 and 0:5.

PS/PU polymer blend fibres of different weight ratios (10:0, 9:1, 8:2, 7:3 and 6:4) were fabricated by dissolving the supplied polymer pellets in DMF/THF (4:1), with the polymer concentration kept constant at 20%w/w. All solutions were stirred using a Stuart Magnetic Stirrer at room temperature for a minimum of 24hrs.

Viscosity was measured with a Melvern Kinexus Rheometer, at 25°C using a shear rate 100-1000rpm. Values reported here represent measurements taken at shear rate of 100rpm.

2.1.1 Electrospinning Apparatus.

A typical horizontal electrospinning configuration was used in this work to generate the mats. The setup comprised a high voltage supply (FC series) Model PS/FC30R04.0-22 (Glassman High Voltage Inc, UK), a programmable syringe pump model 4400PSI (Harvard Apparatus, UK), a 21G needle (BD, UK) connected to a 10ml plastic syringe (BD, UK), and a stainless steel collector covered with aluminium foil. For the polymer blend, the needle tip to collector distance was maintained at 15cm, a precursor flow rate of 3ml/hr was employed, while the voltage was set at 15kV, to obtain stable jet propagation between the needle and the collector. All fibres were air dried in ambient conditions before characterisation or further processing. Figure 1 shows a basic schematic of the mat deposition apparatus.

2.2 Mat Characterisation

In a polymer blend fibre, the structural arrangement of the constituent polymers in the fibre filament will depend upon the intrinsic properties of the pure polymers, such as molecular weight and their miscibility. Additionally, surface tension of the blend precursor solution, miscibility of the solutions (as distinct from the polymers) and the relative weight ratio of the constituent polymers are also strong determinants[18]. Electrospinning a polymer blend could generate any of the following morphologies; a mixture of separately spun fibres, filaments with alternating “zones” of the constituent polymers, or a homogeneously dispersed polymer mix where the polymers in the fibre matrix are still separated but on a scale smaller than the fibre diameter[19]. Clearly the type of mixture generated will have a strong effect on the sorption properties of an electrospun mat, as well as its mechanical properties.

2.2.1 Microstructural and Chemical

Given the earlier stated link between sorption properties and fibre/mat morphology, surface morphology of both individual fibres and fibre mats were investigated using a Field Emission Scanning Electron Microscopy (FESEM), model JSM 7401F (JEOL Limited, Japan), at an accelerating voltage of 2-3kV. Samples were coated with Gold-Palladium using a high resolution beam coater, model 681 (Gatan Ltd, USA). The mean fibre diameter was determined from over 200 measurements taken from two different micrographs using ImageJ software (NIH, USA).

To provide evidence for the existence of both polymer fractions in the resultant mats, ATR-FTIR spectra of all the polyblend mats were recorded using a Spectrum 2 spectrometer (Perkin Elmer, USA). Spectra were acquired at a wavelength range of 400 - 4000 cm^{-1} using a resolution of 4 cm^{-1} and total of 20 scans.

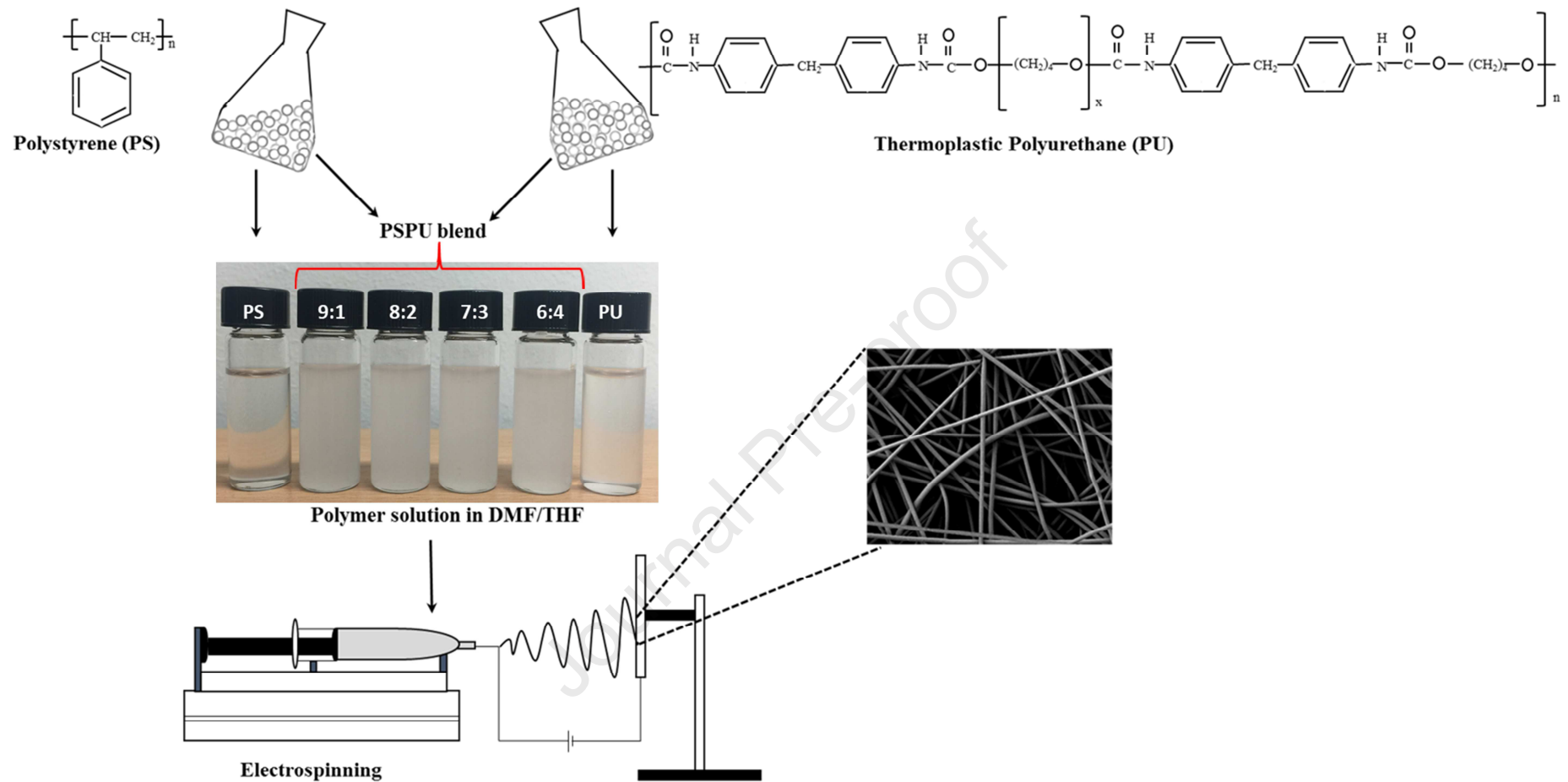


Figure 1: Schematic diagram of the electrospinning setup used in this study.

To help understand whether the blending was on a microscale level (i.e. within individual filaments) or whether only on the macro (i.e. mat) level, Energy Dispersive X-Ray (EDX) Spectroscopy attached to a Hitachi S3400 scanning electron microscope was used to carry out spot elemental analysis of individual fibres in the polymer blend mat. All samples were sputter coated with a carbon layer using a turbo-pumped thermal evaporator K975X (Quorum Technologies, UK). The spot analysis has a scan area of $1\mu\text{m} \times 1\mu\text{m}$ making it possible to focus on individual fibres, as the mean fibre diameter for fibres used in this study falls between $2\text{-}4\mu\text{m}$. Other analysis techniques such as XPS usually have a scan area between $10 - 1000\mu\text{m}$, making it unsuitable for single fibre elemental analysis.

To further study the morphological structure of the fibres, DMT modulus mapping of the polymer blend fibres was performed using Atomic Force Microscopy (AFM) and Peakforce Quantitative Nanomechanical Mapping (PF-QNM). Testing was carried out on a single filament of each fibre using a Bruker Multimode 8 AFM (Coventry, UK). For each analysis, a scan area of $1\mu\text{m} \times 1\mu\text{m}$ or $500\text{nm} \times 500\text{nm}$ was chosen at the top of the fibre filament, depending on the fibre size, at a measuring pixel density of 256×256 . Prior to measurement, the cantilever tip was calibrated through an iterative process using a known reference sample.

Peakforce QNM measures the Young's modulus using the Derjaguin-Muller-Toporov (DMT) model; a modified form of the Hertzian model which takes into account the adhesion between the tip of the cantilever and the sample [22] using equations (1) and (2) below;

$$F_{\text{tip}} - F_{\text{adh}} = \frac{4}{3} E_* \sqrt{R(d^3)} \quad (1)$$

where $F_{\text{tip}} - F_{\text{adh}}$ represents the force on the cantilever relative to the adhesion force, R the radius of the cantilever tip; d is the sample deformation and E_* the reduced modulus. The relationship between the reduced and sample modulus is expressed in equation (2) below;

$$E_* = \left[\frac{1 - \nu_s^2}{E_s} - \frac{1 - \nu_{tip}^2}{E_{tip}} \right] \quad (2)$$

E_{tip} and E_s are the modulus of the cantilever tip and sample respectively, while ν_s and ν_{tip} represents the corresponding Poisson's ratio

To assist with sorption characteristics, water contact angle measurements were taken using a DSA MK-10 contact angle device. A 4 μ l droplet of deionised water was dispensed at different points on the fibre mat. The reported value represents an average of seven measurements.

2.2.2 Thermal and Mechanical Behaviour

Thermal methods were used to characterise fibres given that a blended polymer could exhibit different thermal decomposition behaviour as well as a variation in glass transition temperature distinct from those present in the constituting homopolymer/copolymers. This should allow a measure of the level of polymer miscibility to be obtained. Thermogravimetric Analysis (TGA) was performed using a TGA7 device (Perkin-Elmer, UK) under a nitrogen blanket at a temperature range of 30 - 800°C, and a heating rate of 20°C/min.

The glass transition temperature of both the pure polymer fibres and the blends were measured using a differential scanning calorimeter, DSC Q2000 (TA Instrument, UK). The measurements were performed in a nitrogen atmosphere at a temperature range of -80 to 150°C and a heating scan rate of 10°C/min. The glass transition (T_g) temperatures were analysed using the in-built TA instrument software.

The tensile properties of the polymer blend mats were investigated using a bench type tensile testing machine, model H5KS (Hounsfield Test Equipment, UK), equipped with a 100N load cell and a crosshead speed of 2 mm/min. The tests were carried out with modifications to ASTM D882 test standard. Samples were collected after 30 mins of fibre deposition and each sample had a width of 10mm and a gauge length of 20mm. The modifications to the ASTM standard were necessary to deal with the small size of specimens and their fragility when in mat form. A bespoke gripping arrangement was designed and constructed for the samples, and a clamping protocol, using a removable backing sheet, developed to ensure the specimens were not damaged by insertion into the grips. Sample thickness was estimated from five measurement taken at different points on the mat using a fabric thickness gauge. Tensile values reported represent an average from 5 specimen tests.

2.2.3 Specimen Identification

Unless otherwise stated, specimens were identified by their PS/PU ratio (by mass). Thus PSPU 8:2 refers to a starting composition prior to electrospinning of 80% PS and 20% PU. Two different PU precursors were employed, referred to as PU1 and PU2 (see Section 2.1).

2.2.4 Mat Sorption Properties.

All static and dynamic sorption tests were performed with slight modification to the ASTM F726-12 test standard in order to account for the small specimen sizes that were electrospun. To analyse the oil-water selectivity, under static and dynamic conditions, 20g of oil was added to a 250ml glass beaker containing 150ml of seawater to form an oil layer of approximately 7mm thickness. Approximately 0.15g of the bi-component fibre mat (accurately weighed) was placed on the oil-water medium for 2 mins, after which the wet mat was removed, drained for another 2 mins before weighing again. The sorption capacity was evaluated using equation (3) below[12];

$$\text{Sorption Capacity (SC)} \left(\frac{g}{g} \right) = \frac{m_1 - (m_0 + m_w)}{m_0} \quad (3)$$

Where m_1 is the mass of the wet sorbent after draining, m_0 is the initial mass of the dry sorbent and m_w represents the mass of any sorbed water. In all tests, the amount of water sorbed was found to be negligible, hence m_w was taken as zero. For the dynamic system, the oil-water medium was agitated at 250rpm. Additionally, to aid comparison of the oil sorption capacity of the polyblend mat with previous literature, the tests were conducted using directly comparable oils.

3. Results and discussion

3.1 Morphological characterisation

3.1.1 Preliminary electrospinning test

Preliminary tests were performed to determine the optimum concentration and solvent mix to generate electrospun PS fibre (in terms of uniformity). The use of DMF and THF as solvents for PS has previously been reported in literature[23, 24]. Whilst a previous study on the effect of concentration on fibre morphology was done over a wide range of PS

concentration[25], here a shorter concentration (15%-25%) range was used, in order to capture the critical concentration as well as the morphological transformation more effectively. The DMF/THF ratio was maintained at a mass ratio of 4:1. Fibres produced with a polymer concentration below 20% were observed to have a beaded structure (see Figure S1). The shape of the beads became elongated with increased polymer concentration (15-17.5% PS wt.), while at 20% PS w/w, continuous uniform fibres were obtained. The mean fibre diameter was seen to increase steadily with increasing polymer concentration. This could be ascribed to an increase in the solution viscosity, which in turn causes an increased polymer chain entanglement and a greater resistance to chain stretching, during the jet propagation phase of electrospinning[26].

To investigate the effect of solvent composition on PS fibre morphology, the study was also carried out using DMF/THF ratios; 5:0; 4:1; 3:2; 2:3; 1:4 and 0:5(w/w) respectively. A 20% polymer mass concentration was maintained in all the solvent mixes, an applied voltage of 15kV was used on the ES apparatus with a precursor flowrate of 2ml/hr and a collector distance of 17cm. Fibres produced with a solvent mix of DMF/THF 0:5, exhibited a “collapsed” structure due to the high vapour pressure of THF with small meso/macroporous pores observed on the surface of the fibres (see Figure S2). All fibres produced with a higher level of THF in the solvent mix (i.e. DMF/THF 1:4 and 2:3), were observed to exhibit ribbed and wrinkled like structures respectively. Similar structures have been reported in the literature[25], and could be attributed to the rapid evaporation of THF, being the major solvent in the mix, thereby creating a porous structure and a buckling instability during electrospinning[19, 25, 27]. DMF/THF (4:1) was observed to produce the smallest mean fibre diameter of 1.52 μ m while pure DMF (5:0) produced a uniform fibre structure, in contrast to previous work[25], possibly due to differences in environmental conditions within the electrospinning apparatus.

3.1.2 Morphology of electrospun PS/PU polymer blend mat

The observation in the preliminary study that fibre morphology was greatly dependent on solution parameters such as the solvent mix, solvent properties, and solution concentration, resulted in the optimized solvent mix of DMF/THF (4:1) and solution concentration of 20% (w/w) being chosen, and maintained, in all subsequent PSPU polymer blend production runs. Process and ambient parameters (voltage, flow rate, tip to collector distance, temperature) are regarded, however, to be of lower influence on fibre morphology in comparison to solution properties[26]. An applied voltage of 15kV, nozzle/tip to collector distance of 15cm and a feed rate of 3ml/hr was utilized for the PS, PU and PS/PU polyblend fabrication, given that these settings were observed to produce a stable electrospinning jet in all of the polymer blends.

Figure 2 shows the FESEM micrographs of the nonwoven fibre mat obtained from varying PS/PU polymer blend ratios, indicating the effect of varying the blend ratio on fibre morphology. Mean fibre diameter of the different blends was between 3 - 4 μ m, with the mean diameter showing a gradual increase with increasing PU (PU1) concentration from 3.02 μ m in the pure PS mat to 3.86 μ m in PSPU (6:4) case, with the exception of PSPU 7:3 which showed a slight deviation from the trend. The increasing fibre size could be attributed to the increased viscosity of the blend, which rises with increasing PU content (PU has a higher base polymer

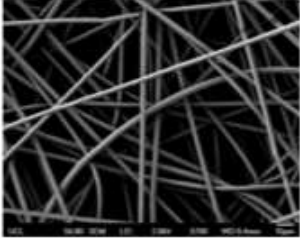
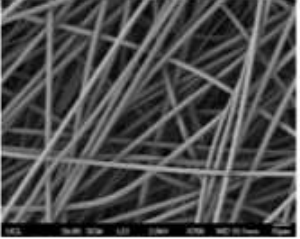
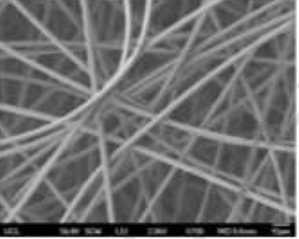
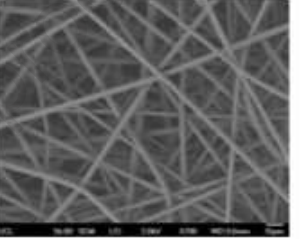
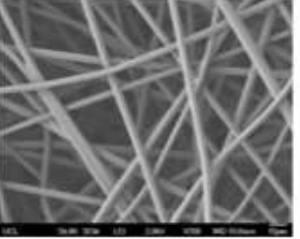
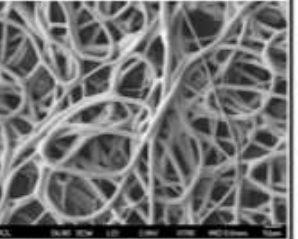
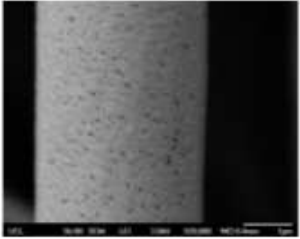
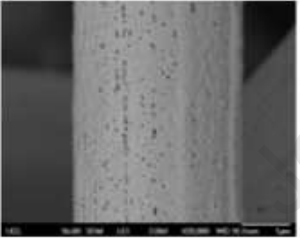
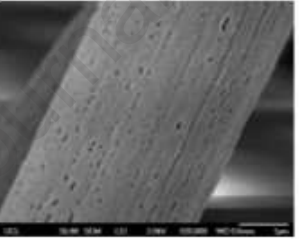
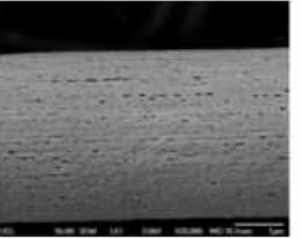
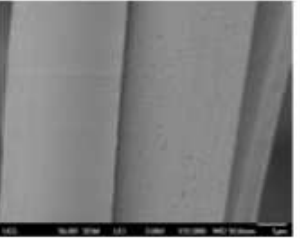
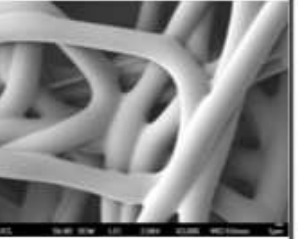
PS/PU1 Polymer Blend (w/w)						
	10:0	9:1	8:2	7:3	6:4	0:10
Low Mag.						
High Mag.						
MFD	3.02 μ m	3.26 μ m	3.56 μ m	3.47 μ m	3.86 μ m	3.46 μ m
Viscosity	0.366Pas	0.496Pas	0.772Pas	1.074Pas	2.253Pas	6.826Pas

Figure 2: FESEM micrograph of the different PPSU1 polymer blend fibres, showing the microstructural attributes of the fibres, average fibre diameter and solution viscosity

density (1.2g/cm^3) than PS (1.04g/cm^3) polymer). The polydisperse nature (in terms of fibre diameter) of the pure PU fibre was probably a result of the unsteady nature of the jet at the optimized parameters used for the blend.

Significantly, meso- and macroporous pore structures could be seen on the surface of the PS fibres and on the polymer blend fibres with a high PS ratio. This was believed to be a result of the less dense PS polymer enabling the process of vapour and thermally induced phase separations (VIPS and TIPS)[28] - during the electrospinning process, VIPS occur when low boiling point solvents such as THF evaporate rapidly from the spinning polymer jet leading to a drop in temperature (through evaporative cooling), along the surface of the jet[15, 29]. This causes ambient water vapour to condense on the surface of the polymer and subsequently form pores upon evaporation. Such pore structure, however, could enhance the specific surface area available for oil adsorption. An increase in the higher density PU in the blend, as seen in ratio (6:4), slows down the rate of solvent evaporation leading to a reduction in pore formation as well as the appearance of inter-fibre bonding. This is more evident in the pure PU fibre mat.

To study the effect of solvent composition on the polymer blend, PSPU1 (8:2) was dissolved in pure THF and pure DMF respectively, using the optimized parameters as given in Section 2.1.1. In pure DMF, multi-jetting and rapid jet instability was observed during the electrospinning process at the applied voltage of 15kV, while a reduction in applied voltage to 10kV resulted in single and stable jet propagation. The high dielectric strength, dipole to dipole moment and surface tension of DMF, is known to increase the solution conductivity[29, 30], hence the instability observed in the pure DMF solution at 15kV was mitigated by reducing the applied voltage and Figure 3a shows the SEM micrograph of a uniformly distributed fibre mat so obtained. The mean fibre diameter (MFD) is $3.17\mu\text{m}$. Figure 3b shows a more polydisperse (and hence undesirable) fibre mat generated at the

higher applied voltage (15kV) with an MFD of 2.60 μ m. The behaviour in pure THF was noticeably different, with the electrospinning process generating stable jetting over a wide range of applied voltages studied (10-15kV). The polymer was, however, observed to dry up rapidly at the tip of the needle due to rapid THF evaporation. A similar effect has been reported in the literature[25, 29], and can be attributed to the low boiling point and surface tension of THF. Figure 3c shows that the fibres were similar to those produced from pure PS polymer dissolved in THF only solvent (as seen in Figure S2f).

3.2 Hydrophobicity/Oleophilicity

As discussed above, a key desirable property of an oil sorbent is its oil-water selectivity and in order to evaluate the hydrophobic-oleophilic property of polyblend mats, 2 μ l droplets of both of oil and water were applied to each mat. In all cases, the oil was seen to spread out and penetrate into the mat through the inter fibre void spaces almost immediately. Conversely, as expected, water droplets remained on the surface throughout the observation period of 20 minutes, as can be seen in Figure 3d for the PSPU 8:2 mat. This is an indication of the affinity of the polyblend fibre for oil (i.e. its oleophilicity), and of a commensurate repulsion for water (i.e. hydrophobicity). Figure 3e, shows that irrespective of the water droplet size, the polymer blend mat remained hydrophobic. Water Contact Angle (WCA) measurements confirmed the hydrophobicity of the polyblend mat, as all WCA values were found to be above 90°. The variation of WCA with blend composition is shown in Figure 3f. The WCA values of pure PS and PU1 fibres are approximately equivalent, however it can be seen that a modest rise (approx. 10%) in WCA was observed in a number of the mats fabricated from the blended polymers. This is a significant observation as it suggest hydrophobicity (and concomitant oleophilicity) [31] which is greater than the sum of its parts. This could be interpreted as a synergistic effect present in the blended polymer fibres. As

postulated above however, sorption capacity is likely to be a complex function of bulk properties and morphological factors, including fibre

Journal Pre-proof

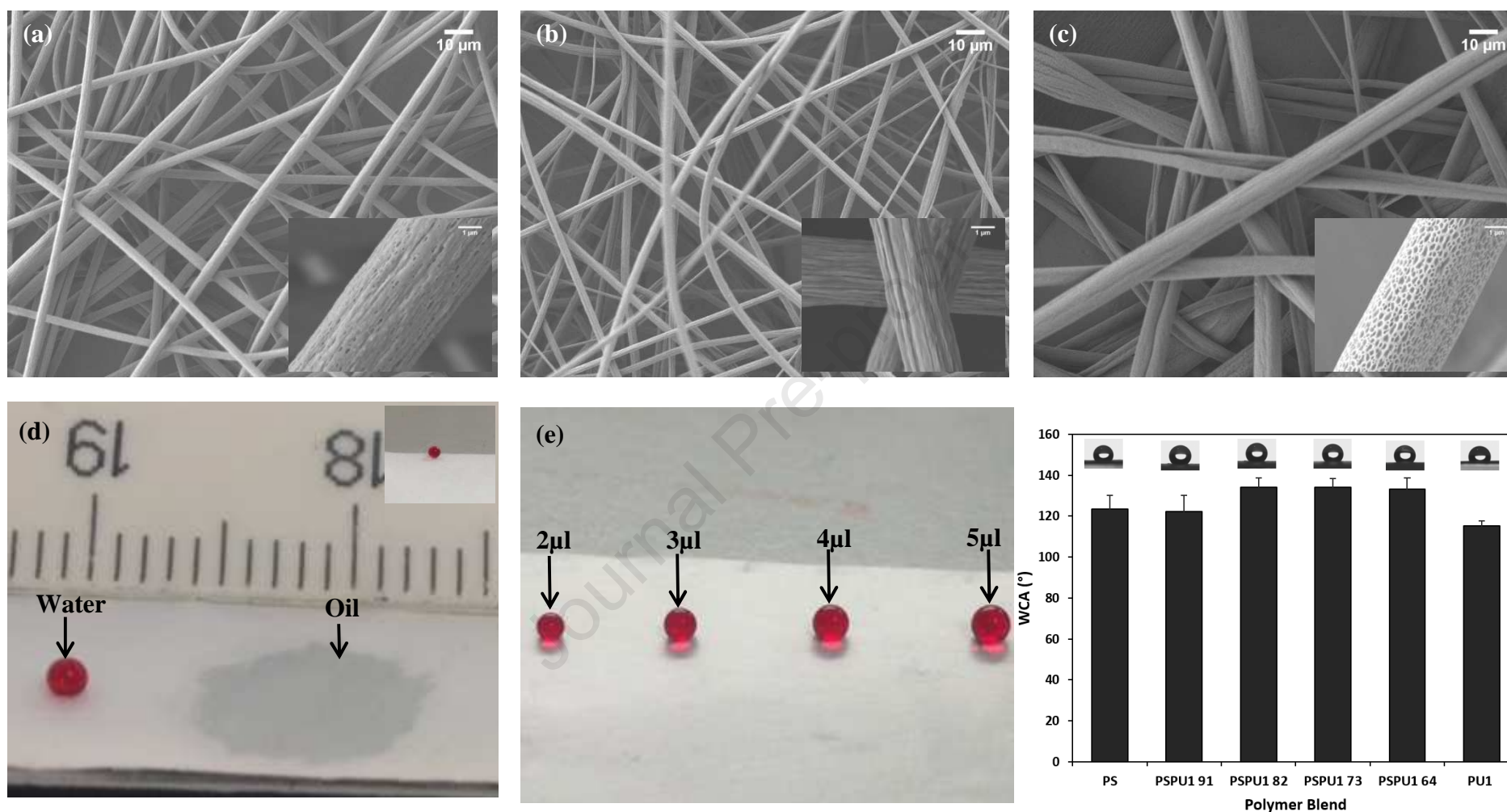


Figure 3: FESEM micrograph of 20% PSPU1 (8:2) dissolved in DMF with applied voltage (a) 10kV (b) 15kV; (c) micrograph of 20% PSPU1 (8:2) dissolved in pure THF at 15kV(d) water dyed with red food colouring and vegetable oil droplets on PSPU1 (8:2) fibre mat (e) different water droplet size on the same fibre mat all exhibits hydrophobicity (f) illustrate the WCA for the different pure and polyblend fibre mats of PS and PU polymers

(i.e. micro) and mat (i.e. macro) morphology. Thus the rise observed in WCA could also be ascribed to these latter factors. In particular, the high magnification images of fibres in Figure 2, do show high levels of meso- and macro- level porosity, which is not otherwise present in the PU1 fibres. In addition, the interfibre void spaces between the polymer blend fibres appears less compacted in comparison to the PU1 fibre mat. These are significant observations, as the structure of a porous material is known to play a key role in its hydrophobicity[32, 33]. Similarly, there are strong differences in the mat morphology.

3.3 ATR spectroscopy of the fibre mat

Understanding the chemical composition of the polymer blend fibre mats should give an insight into the origin of their hydrophobicity, as well as provide confirmation that both polymers exist in the electrospun mat. For example, the presence of CH₂ and CH₃ functional groups have been associated with hydrophobicity in previous studies[34]. Figure 4 displays the ATR-FTIR spectra of electrospun PS, PU1 and PSPU1 blend mats. The spectra for the pure PS mat clearly shows the characteristic absorbance peaks of the aromatic C-C bond stretching at 1493 and 1452cm⁻¹, benzene ring vibration at 1074cm⁻¹; C-H out of plane bending vibration at 756cm⁻¹, while the prominent band at 697 cm⁻¹ can be attributed to the CH₂ rocking mode[35, 36]. The CH and CH₂ stretching vibration of the main PS chain was observed at 2849 cm⁻¹ and 2922 cm⁻¹ respectively. The crowded spectra observed for pure PU fibre in the short wavelength band is due to the complex molecular structure of the polymer[37]. In the pure PU spectra, the distinctive peaks for the stretching vibration of N-H group was observed at 3325cm⁻¹, the asymmetric and asymmetric stretching of methylene groups (CH₂ and CH₃) at 2939, and 2854cm⁻¹, while the peaks at 1731 and 1700cm⁻¹ can be ascribed to the stretching vibration of the non-bonded and bonded carbonyl (C=O) group[37, 38].

In the PSPU1 polyblend mats, the presence of absorbance peaks that can be ascribed to pure PS and PU1 polymers (as indicated with arrows (Figure 4)), confirms the formation of a bi-component mat structure which contains both polymers within the mat. It is recognised, however that this says little about how these polymers are combined and importantly whether or not this occurs at the fibre level.

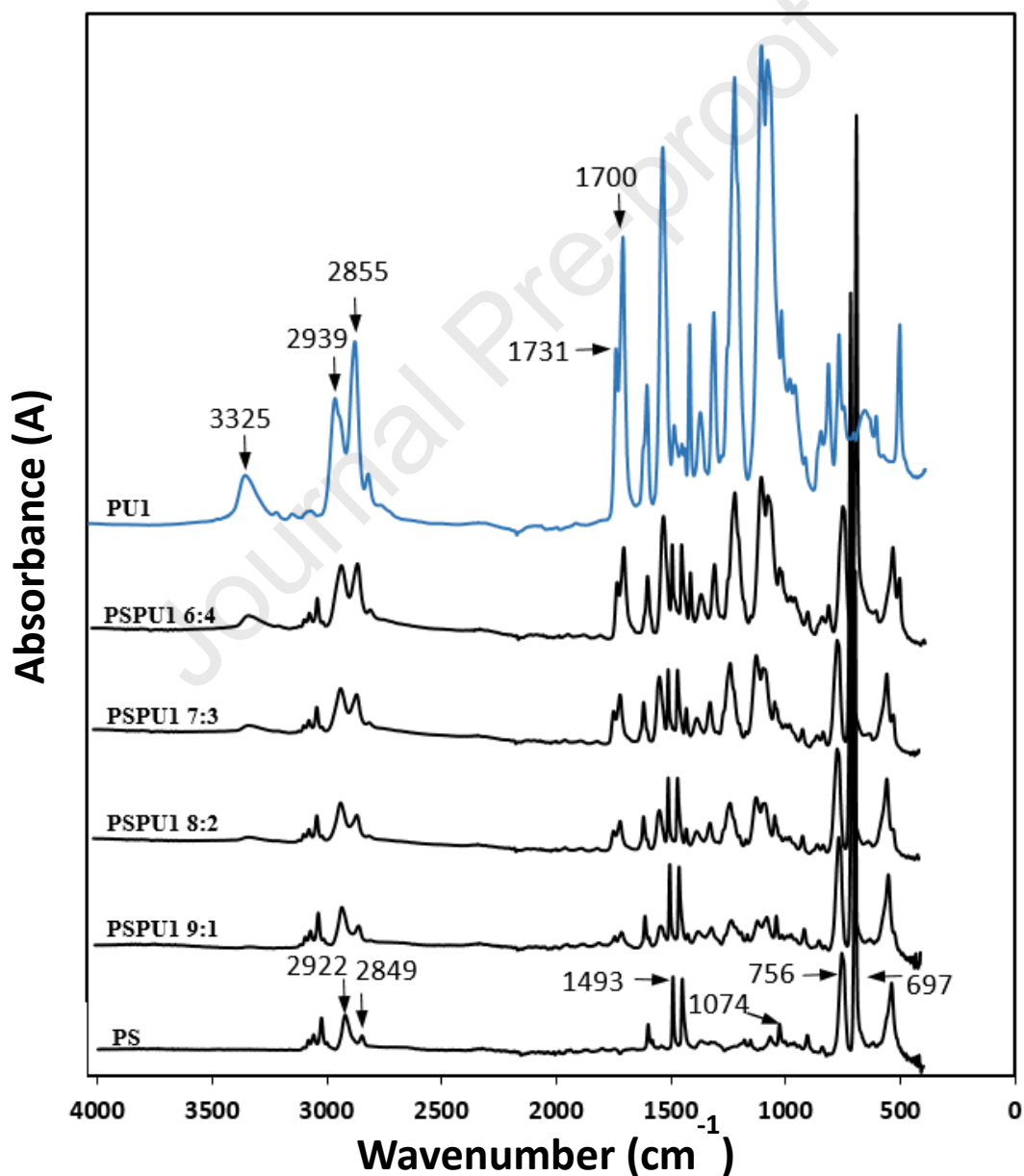


Figure 4: ATR-FTIR spectra of pure PS, pure PU1 and PSPU1 polymer blend fibre mat. Peaks of the pure polymer that can be distinctly observed in the polymer blend are indicated with the red arrow

3.4 EDX and AFM (PF-QNM) Analysis of the fibres

Secondary electron (SE) and backscattered electron (BSE) images of the pure PS, pure PU1 and the PSPU1 (8:2) polymer blend mat, are shown in Figure 5 (a-c) and (a`-c`) respectively. There were no signs of segregation of the different polymers in the case of the PSPU1 (8:2) fibre mat. This could be deemed a confirmation of an intra-fibre blended structure, given that BSE imaging has the ability to detect elemental differences at sample surfaces and at a sub-surface level. Elemental point (spot) analysis was therefore conducted at three different regions along the length of a single fibre filament. As the chemical structure of polystyrene $(C_8H_8)_n$ comprises solely of carbon (C) and hydrogen (H), it is not surprising to see the spectra from the PS fibre (in Figure 5a`) reveal only the presence of C (in addition to Al from the aluminium substrate). The spectra from one of the pure PU1 fibres is given in Figure 5c`, and this shows an O atom peak, in addition to C. Similarly, spectra from the polymer blend fibres also indicated traces of O (see Figure 5b`), and significantly, the intensity of the O peak in the blended fibres, was observed to increase with increasing ratio of PU in all the ratios studied (results not shown).

These results were encouraging as they strongly implied that co-spinning polymers from a single nozzle (as opposed to side-by-side multi-nozzle or coaxial electrospinning) resulted in a *microscale* integration of the polymers (i.e. at the intrafibre level), and possibly at the nano level[18]. Such close mixing could give rise to fibres which will combine properties from both polymers, nominally under a simple rule-of-mixtures regime but also possibly generating synergistic interactions which, in turn, could create new and unexpected thermal and mechanical properties in the fibres, and hence in the mats.

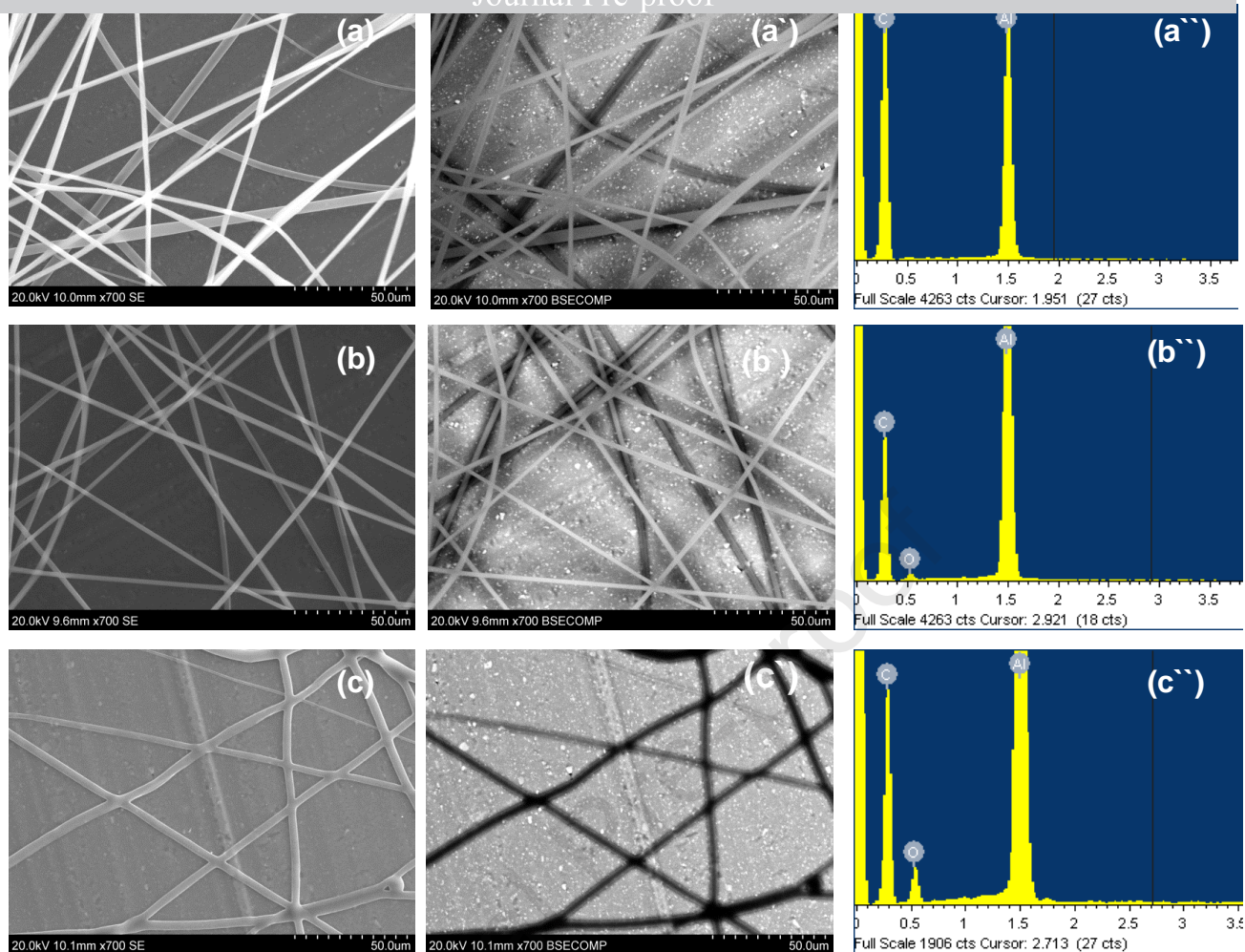


Figure 5: (a - c) Shows secondary electron image of pure PS, PSPU1 (8:2) and neat PU1 electrospun fibres respectively, while (a'-c') and (a''-c'') shows the corresponding backscattered and EDX spectra of the fibres.

Results from AFM Peakforce Quantitative Nanomechanical Mapping (QNM) further strengthen the assertion that the polymers mixed well. The technique is capable of providing both micro/nano morphological information and mechanical properties of materials. The use of modulus mapping for the morphological study of polymer blends has been widely reported in the literature[39, 40] as it offers excellent spatial resolution, at a cost effective and faster rate in comparison to other morphological analysis methods such as transmission electron microscopy (TEM) [41]. The DMT modulus imaging of individual fibre filaments revealed no phase segregation in the PS/PU polymer blend fibres as shown in Figure S3 (a-f). This is in spite of the large difference in DMT modulus of the constituent polymers (2.9GPa for pure PS fibre and 0.34GPa for PU1 fibre). The lighter shade areas, as seen in images of both the

PS and PS/PU polymer blend, can be ascribed to the uneven surface of the electrospun fibres used in this analysis, as can also be seen in the 3D height images in Figure S3(g-k).

Journal Pre-proof

3.5 Thermal Analysis

The results of the thermal degradation measurements of pure PS, PU1 and PSPU1 polymer blend fibres are summarised in both the TGA and DTGA thermographs in Figure 6a and 6b and in Table 2. The pure PS fibre mat exhibited a one-step thermal degradation with a single transition temperature, while the pure PU1 mat showed a two-step decomposition profile (see insert in Figure 6a). The first and second stage degradation of pure PU1 fibre can be attributed to the decomposition of the polymer hard and soft-segments respectively[42], (as expected in a typical thermoplastic elastomer). The hard-segment degradation reaches a maximum at 369.4°C and the polymer completely degrades by 397.5°C. This amounts to approximately 45% of the mass of the hard-segment in the PU1 composition. At the same temperature (397.5°C), only 7% degradation is observed in a pure PS fibre mat. Both pure PS and PU1 exhibits the same weight loss (77%) at 433.3°C. Based on these observations and on the onset of decomposition of pure PS and PU1 polymer mats (as additionally shown in Table 2), it can be inferred that PS mats exhibit a higher thermal stability than their pure PU1 counterparts.

Turning to the mats fabricated from blended polymers (Figure 6b), all were observed to exhibit a two-stage degradation profile. This is further confirmation of the presence of PU in these fibrous mats. Interestingly, the onset of thermal decomposition of the blends occurs at much lower temperature than those obtained for the pure polymer cases, while the peak degradation temperature (with the exception of PSPU1 6:4) was between those of the two pure polymers. This is possible evidence for a synergistic interaction between the two polymers at the fibre level, rather than a simpler rule of mixtures relationship. Similar effects was reported for a PLA/PS polymer blend in the literature[43].

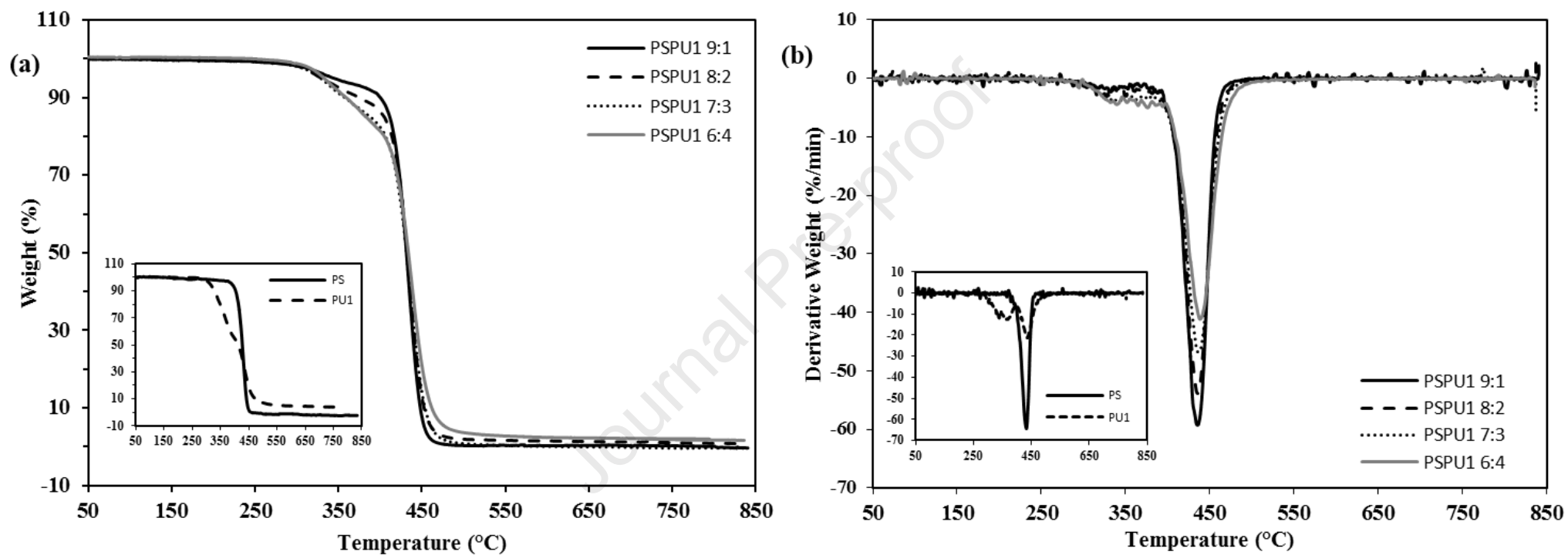


Figure 6: (a) TGA and (b) DTGA curves of electrospun PS/PU1 polymer blend fibres. Insert (a) TGA and (b) DTGA of pure PS and PU1

The position of the glass transition (T_g) temperature in a binary polymer blend, relative to the T_g of the pure polymer, is often used to determine the level of miscibility of the polymers in the blend. As a rule, polymer blends characterised by a single glass transition temperature which falls in between the T_g values of the constituent polymers are said to be miscible[43, 44]. A partially miscible blend has two distinct T_g values which are composition (ratio) dependent, while an immiscible blend is characterised by two separate T_g values which are the same as those of the pure constituent polymers[45]. Figure 7 is a summary of the DSC thermographs of electrospun PSPU1 polyblend fibres, at the various blend ratios.

The glass transition temperature for the neat PU1 and PS fibre was observed at 40.5°C and 114.7°C respectively, which is consistent with previous work[43]. In all the polymer blends, however, the thermographs show a distinctive, single transition, temperature which falls between those of pure PS and PU1 polymer. It should be noted however that a bimodal exothermic transition was observed for the PS fibre which could be the effect of the high voltage (during spinning) causing some structural changes in the PS fibre, given the same transition was observed in repeated runs of the PS fibre.

Notwithstanding the bimodal PS behaviour, these results are further evidence that there is a strong interaction and concomitant good miscibility between the two polymers. Such a degree of blending can often be used to a great effect in allowing materials to be “engineered” to achieve a specific set of desired properties – or to even exhibit new or amplified properties if any synergistic effects occur[45].

3.6 Tensile properties of the polyblend mat

An ideal sorbent, particularly for marine oil spill clean-up, should have a relatively good mechanical strength [46] and maintain its structural integrity during and after oil sorption so as to aid subsequent removal and disposal. The mechanical properties of an electrospun polymer blend is expected to be dependent on the intrinsic properties of the constituent polymers, the ratio of these polymers, and their degree of interaction in the blend, as well as the structural orientation of the fibres and the existence of inter fibre bonding in the mat[47]. Tensile tests were therefore performed on various PS and PU1 combinations to study the effect of the addition of the thermoplastic polyurethane on the mechanical properties. A second thermoplastic PU (PU2) was also employed in the mechanical property study, as the manufacturer`s datasheet suggest a higher mechanical strength than PU1, which potentially provided a way of deconvoluting any strength contribution from polyurethane per se. Figure 8a shows a graphical representation of the average tensile strength taken from five samples, while analysis of the mechanical properties is presented in Table S1.

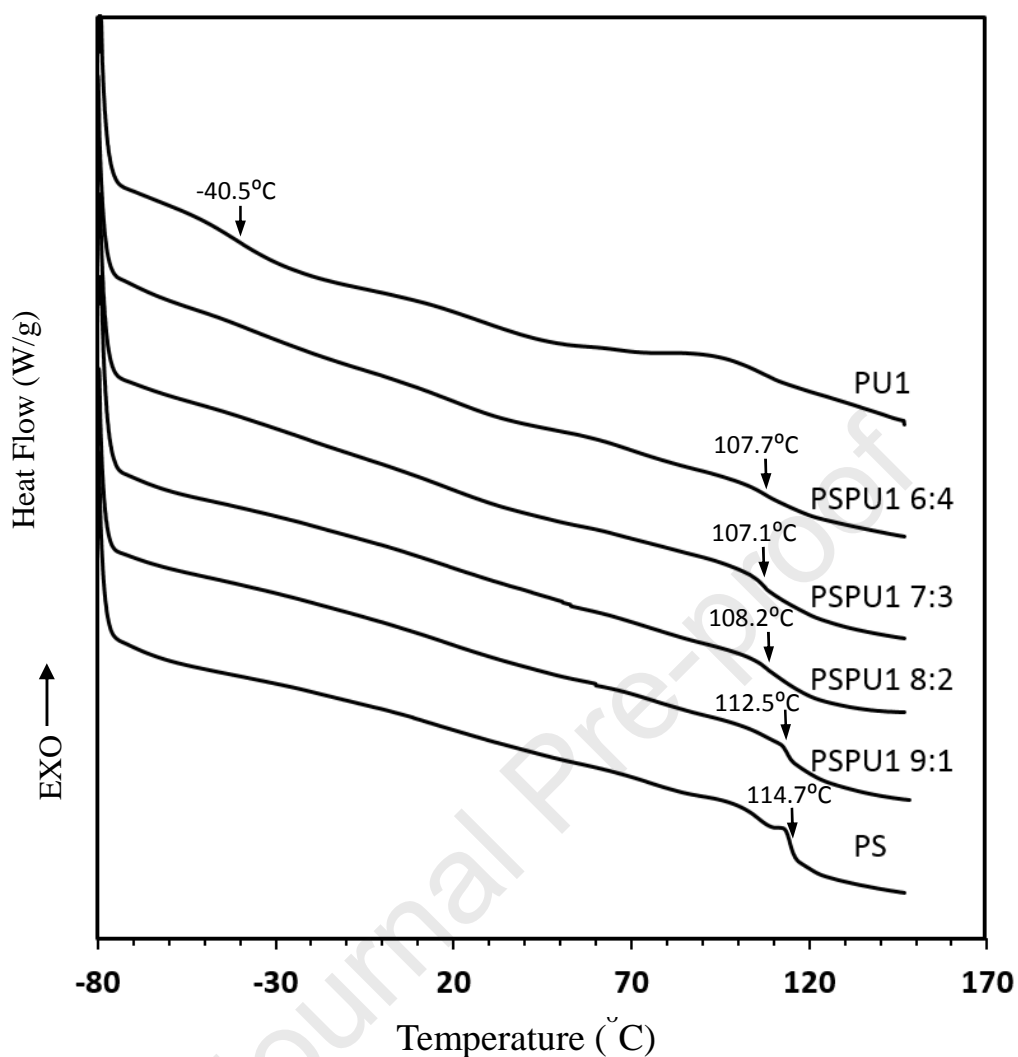


Figure 7: DSC thermograph obtained from PS, PU1 and PSPU1 polymer blend fibres

Table 2: Glass transition temperature (T_g), temperature at onset of decomposition (T_d onset) and

Polymer Solution	T_g ($^{\circ}\text{C}$)	T_d onset ($^{\circ}\text{C}$)	T_d ($^{\circ}\text{C}$)
PS	114.7	412.5	433.2
PSPU1 (9:1)	112.5	292.9	435.3
PSPU1 (8:2)	108.2	298.4	436.2
PSPU1 (7:3)	107.1	299.6	436.0
PSPU1 (6:4)	107.7	302.1	438.5
PU1	-40.5	314.9	436.3

decomposition peak temperature (T_d) for electrospun PS, PU1 and PSPU1 polymer blend fibres

From Figure 8a, it can be seen that the pure PS mat exhibits a low tensile strength of 0.06 ± 0.01 MPa with an elongation at the UTS of 21.06 ± 6.4 %. The addition of thermoplastic polyurethane into the PS matrix saw the tensile strength increase steadily with an increase in PU ratio, to 0.62 ± 0.07 MPa in PSPU1 (6:4) and 1.26 ± 0.43 MPa in PSPU2 (6:4). This represents a 933% and 2000% increase respectively from the pure PS fibre mat. Data for a pure PU mat is not presented here as the experimentally produced mats were much denser and flatter than for the polyblend constituent, at the optimised process parameters. However, the results of the polyblend test clearly shows a marked improvement in strength with increasing PU content. The increasing trend in mechanical properties could be attributed to the formation of interfibre bonds as a result of PU additions. The authors cannot discount the possibility of an improvement in *individual* fibre strength via interactions between molecules of both polymers, at a micro/nano level. However, similar interfibre bonding has been reported for PVC/PU polymer blends[47] which tends to support this as the predominant mechanism. Figure S4, shows a typical stress strain curve for PS and PSPU1 polymer blend mat. The PS fibre mat is seen to exhibit a non-linear elastic behaviour in the first stage of the plot, most likely due to fibre slippage and the absence of interfibre bonds. This changes with the addition of PU1 into the polymer matrix, with a more distinct elastic behaviour in the first stage and an increase in UTS observable with increasing PU1 addition. The changes in the mechanical behaviour of the mat can be attributed largely to the interfibre bonds that PU adds to the mats, as clearly illustrated in Figure S4. The presence of inter-fibre bonds increases with PU addition and was observed to be greater in PSPU2 64 in comparison to PSPU1 64, which could be the reason for the higher UTS observed (see Figure 8). In addition, a lower mean fibre diameter of $2.64\mu\text{m}$ was recorded for PSPU2 64 in comparison to $3.85\mu\text{m}$ recorded for PSPU1 64. This could also be the reason for the higher UTS[48], as previous

studies have shown that a decrease in fibre diameter results in both higher modulus and higher UTS[49].

To help clarify the origin of the rise in strength, SEM micrographs of mats were recorded after tensile testing and these can be compared to the mats prior to testing. In Figure 2 and Figure 8b, the PS/PU 6:4 ratio fibres do show some evidence of interfibre links. Figure 8c shows plastic deformation of the polyblend fibre after tensile testing, with a number of localized fractured points observed along the twisted fibre filaments. A significant reduction in the average fibre diameter of about 50% ($3.89\mu\text{m}$ to $1.96\mu\text{m}$) was observed between micrographs before and after mechanical testing, as illustrated in Figure 8d. This shows that aside from the visual evidence of interfibre bonding, deformation and yielding is present. Such yielding could only occur if interfibre bonds existed, else the fibres would have slipped easily over each other, rather than resist the load. Comparison with failed PS fibre mats (see Figure S6) shows slight deformation with no localized fractured points on the fibres. Fibres were also seen to align along the axis of pull, suggesting mat failure was predominantly via the relative slippage of the fibres.

Maintaining the stability and integrity of a sorbent during an oil spill clean-up is essential, as often times sorbent recovery (after sorption) is not immediate. To investigate the stability of the polymer blend in oil, the blend with the highest mechanical strength (PSPU2 6:4) was selected for further study. Mats were immersed in a light crude oil and the previous tensile measurements were repeated at various time intervals. Figure 9a and b shows the average tensile strength and a typical stress-strain curve, respectively, of individual fibre mats taken at 0, 18 and 42 hrs of immersion. All fibre mats, under each condition, exhibited a substantial level of linear elastic behaviour followed by a region of plastic deformation. The tensile stress reduced by approximately 50% (from 1.07 ± 0.06 MPa without immersion) to $0.55 \pm$

0.01 MPa after 42 hrs of immersion, while an increase in permanent elongation of about 150% was observed in the same mat sample. The observed increase in “plastic” behaviour coupled with the decreasing tensile strength with period of immersion, could be ascribed to the absorption of the lower molecular mass constituents of

Journal Pre-proof

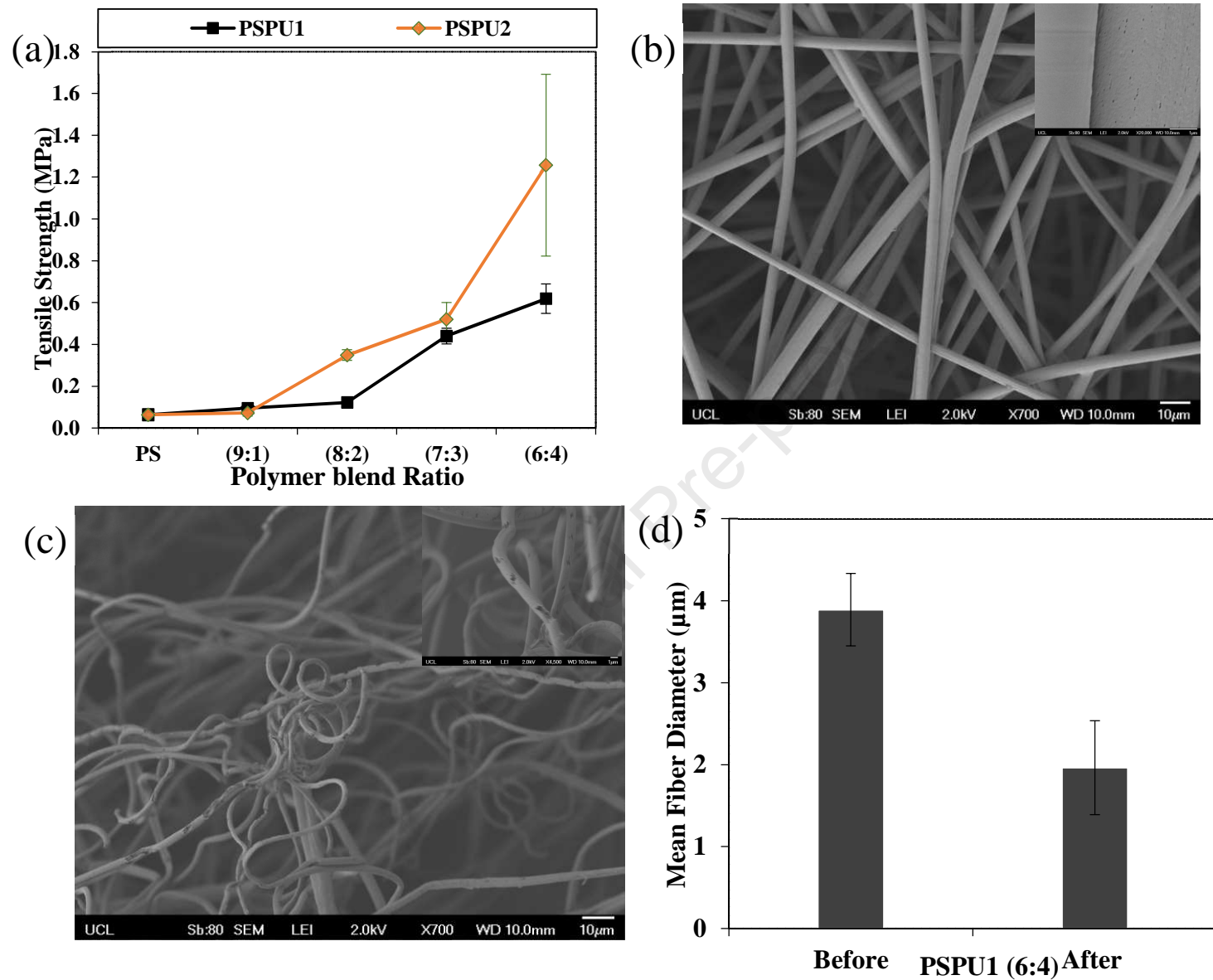


Figure 8: Tensile strength of PS and PSPU1 polymer blend fibres (b) SEM thermograph of PSPU1 6:4 fibre mat before tensile test (c) Sample from same mat after test, (d) Average fibre diameter before and after failure

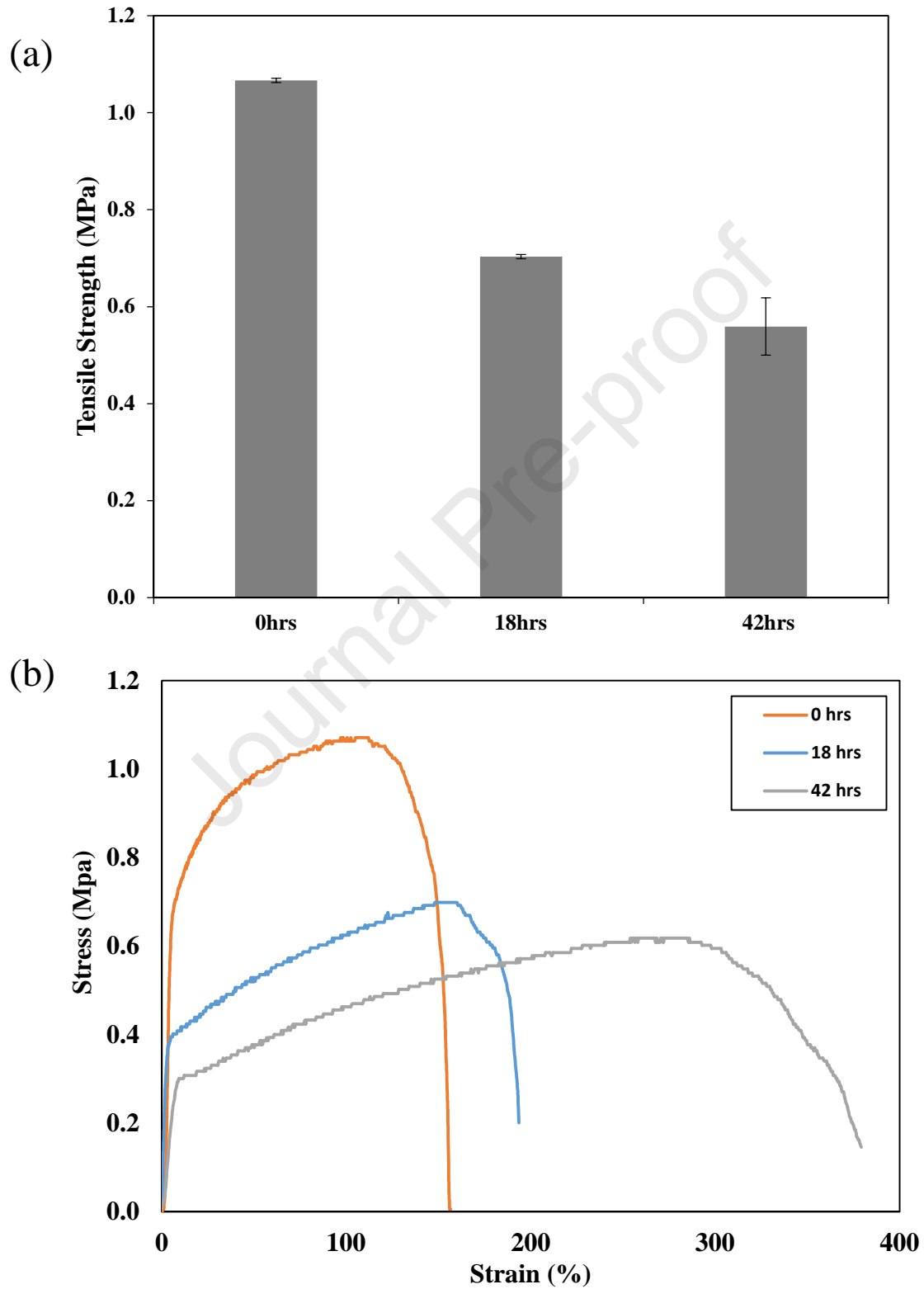


Figure 9: (a) Average tensile strength of electrospun PSPU2 (6:4) fibre immersed in light crude oil over 18hrs and 42hrs (SD n=5) (b) typical stress-stress curve from samples test in (a).

crude oil potentially causing plasticization of the fibre, hence affecting fibre properties. The observed mechanical strength of the blend after 42hrs of immersion still remained higher than that obtained for the pure PS fibre mat – suggesting that interfibre crosslinks remained in place, and that it was a change in fibre properties, per se, that generated the drop in strength. Detailed analysis of the mechanical testing is presented in Table S2.

It is clear from the mechanical testing that the addition of PU to PS, by blending prior to electrospinning, produces a greatly improved mat based product, when compared to a pure PS version, and that this improvement is almost definitely due to an increase in interfibre bonding.

3.7 Oil sorption capacity of the polyblend mat

The improvement in mechanical properties and the enhancement in contact angle suggested that the PSPU 6:4 ratio might be an optimum combination for oil sorption. However, the sorption capacity of a mat is likely to be a complex multi-variable ‘property’. Accordingly, the sorption behaviour of the various PSPU polymer blend mats was investigated in an oil-water system as described in section 2.2.3, using light crude and vegetable oil. Due to the hydrophobic nature of all the blended fibre mats and, as previous work had reported no difference between the sorption capacity in pure oil and in an oil-water system[12], the sorption behaviour in oil-water was used to determine the maximum oil sorption capacity of the different mats. This is much closer to the conditions that might be encountered “in-field”.

Figure 10a shows oil sorption capacities (SC) for the PS and PSPU1 polymer blended mats under static conditions. The SC of the pure PS fibre mat was 80.49g/g and 42.50g/g for vegetable and crude oil respectively. An addition of 10% PU1 into the polymer matrix (PSPU1 9:1) saw an increase in SC for both oils (16.7% in Vegetable oil and 5.5% in crude

oil). Interestingly, further increase in the PU1 ratio in the blend, saw a gradual decline in the sorption capacity. The initial rise in sorption behaviour as observed for PSPU1 (9:1) could be due to the previously observed ability of the PU1 to give some structural integrity via the formation of interfibre crosslinks, which could prevent the collapse of interfibre void spaces. Such spaces would act to capture and hold onto oil. It could also be due to the start of the improvement in WCA (as discussed above), leading to better oleophilicity[31]. The observed subsequent reduction in sorption capacity could (ironically) be due to the same inter-fibre bonding, which could either reduce the available void spaces, or hinder the expansion of the mat as oil is sorbed – again limiting the capacity to hold oil. Figure S5 shows the presence of interfibre bonds in both PSPU1 64 and PSPU2 64 fibre mats. This effect eventually dominates over the improvement in WCA, hence creating a peak in sorption capacity at the lower PU ratio. The reduced or absence of meso- and macro-porous structure on the surface of fibres with a higher PU ratio could also lead to lower surface area for oil adsorption (See figure 2), hence the observed reduction in SC with increasing PU addition.

The higher sorption capacity observed for vegetable oil could be attributed to the higher viscosity of the oil, which enhances the molecular interaction between the oil and the fibre filaments. Generally, a high viscosity oil introduces either an increase adherence to the fibre or a decrease in the ability of the oil to infiltrate the void spaces between the fibre filaments [9, 12] thus, in this case, an argument based on adherence would fit the data better. The same trends in sorption behaviour were observed under dynamic conditions, as seen in Figure 10b (at 250rpm), but with lower sorption capacity in all mats. Similar trends under static and dynamic conditions were observed for PSPU2 fibre mats (in result not shown). The possibility exists that under dynamic conditions, oil already sorbed is displaced due to the agitation, hence the importance of dynamic testing.

Figure 10c and 10d, show a comparison between the sorption capacity of the PSPU polymer blend mats reported in this study with those of previous studies in the literature. The maximum recorded data for coaxial[16] and multinozzle[17] side-by-side electrospun mats of PS and PU polymers is given. Generally, it can be seen from the figure that the PSPU polymer blend mats produced in the present work exhibit a sorption capacity 2 - 5 times higher than those obtained in the reported literature, consistent with the notion that blending rather than co-spinning is more effective for application to sorption mats. It should be noted that this comparison was made using motor and sunflower oil with same test duration to maintain compatibility with the literature[16, 17]. The SC under these oils follows a similar pattern to the results reported for vegetable and crude oil (In Figure 10a and 10b), with PSPU2 (9:1) recording the highest sorption values of 144.52g/g and 110.89g/g in motor and sunflower oil respectively, while PSPU1 (9:1) recorded the highest SC of 123.88g/g and 123.95g/g respectively in the same oil type. The fundamental mechanism(s) for the improved sorption capacity of the present polymer blend mats is not absolutely clear, however it is probable that the electrospinning of a blend, as opposed to coaxial and multinozzle side-by-side electrospinning of two individual polymers, is at the heart of these differences. On the basis of the evidence presented, it is likely that the fibres are formed from intimately mixed polymers, thereby generating a greater homogeneity in properties, as well as the possibility of synergistic effects which overall act to improve sorption behaviour.

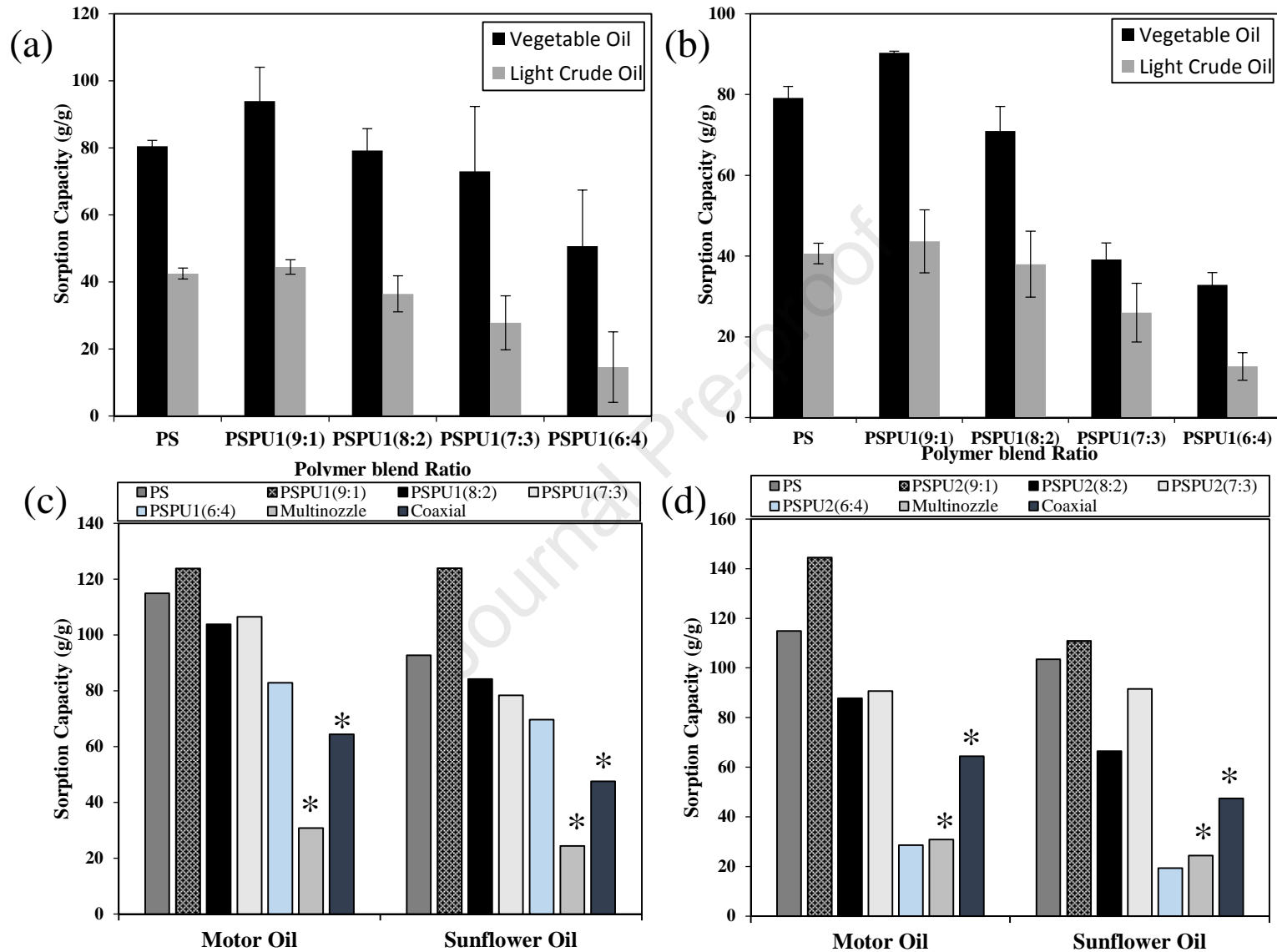


Figure 10: Sorption capacity of PSPU1 fibre under (a) static condition, (b) dynamic condition at 250 rpm, (c) comparison of maximum sorption capacity of PSPU1 with coaxial and multinozzle mats from literature (with asterisk), (d) same as (c) but using PSPU2

4. Conclusion

Polymer blend fibre mats of different PSPU weight ratio were successfully electrospun in DMF/THF (4:1) under laboratory conditions. Microstructural properties of the individual fibres were seen to be dependent upon the relative polymer ratio, solvent composition and applied voltage. Morphological characterisation revealed that fibres produced at optimized parameters (flow rate 3ml/hr, voltage of 15kV and TCD of 15cm) exhibited an AFD between 3-4 μ m, with macro and mesoporous pore structures on the polymer blend fibres. ATR-FTIR and EDX analysis showed the successful formation of a bi-component fibre mat, with EDX elemental spot analysis confirming the presence of a bi-component structure down to a single filament level. DSC provided further evidence that strong miscibility exists between the two polymers at the fibre level, with the creation of a single glass transition temperature. Uniaxial tensile strength measurements showed that the addition of PU in the blend improved the mechanical properties of the mat, while causing a gradual reduction in the oil sorption behaviour potentially as a consequence of tighter packing of the fibres or greater restriction in the fibre freedom. Nevertheless, the polymer blend fibre reported in this study exhibited a sorption capacity 2–5 times higher than those reported in the literature for coaxial and multi-nozzle spinning of PS and PU polymers, a fact which easily mitigates the reduction in the absolute sorption behaviour with increasing PU content. All sorption capacities were at a practicable level for the mats produced.

Overall, this study suggests that there is an optimum blend of PS and PU, especially when “practical” sorption capacity is considered. This will be a function of many different factors which include oleophilicity as well as mechanical behaviour and integrity in the field, so seeking out a “sweet spot” of properties is a highly likely outcome if a commercially viable product is the end goal.

CRedit

Muftau J. Akanbi: Conceptualization, Methodology, Investigation, Writing – original draft

Suwan N. Jayasinghe: Supervision, Project administration, Resources

Adam Wojcik: Writing – review & editing, Supervision, Validation, Resources

Acknowledgements

M.J.A wishes to thank the Petroleum Technology Development Fund (PTDF), Nigeria for funding his doctoral research. The authors will also like to thank Dr Asma Buanz of UCL School of pharmacy for the use of DSC device, Mark Turmaine of UCL biosciences for the FESEM analysis and Dr. Tom Gregory of UCL Archaeology for the EDX analysis. Lastly, our appreciation goes to Lubrizol Advanced Material for providing the Thermoplastic Polyurethanes used in this study.

Funding: This research did not receive specific grant from funding agencies in the Public, commercial, or not-for-profit sectors.

References

1. Cojocaru C, Macoveanu M, Cretescu I: **Peat-based sorbents for the removal of oil spills from water surface: Application of artificial neural network modeling.** *Colloids Surfaces a-Physicochemical Eng Asp* 2011, **384**:675–684.
2. Wei QF, Mather RR, Fotheringham AF, Yang RD: **Evaluation of nonwoven polypropylene oil sorbents in marine oil-spill recovery.** *Mar Pollut Bull* 2003, **46**:780–783.
3. Wang Z, Ma H, Chu B, Hsiao BS: **Super-hydrophobic modification of porous natural polymer “luffa sponge” for oil absorption.** *Polymer (Guildf)* 2017, **126**:470–476.
4. Al-Majed AA, Adebayo AR, Hossain ME: **A sustainable approach to controlling oil spills.** *J Environ Manage* 2012, **113**:213–227.
5. Pan Y, Shi K, Peng C, Wang W, Liu Z, Ji X: **Evaluation of hydrophobic polyvinyl-alcohol formaldehyde sponges as absorbents for oil spill.** *ACS Appl Mater Interfaces* 2014, **6**:8651–8659.
6. Carmody O, Frost R, Xi Y, Kokot S: **Adsorption of hydrocarbons on organo-clays-Implications for oil spill remediation.** *J Colloid Interface Sci* 2007, **305**:17–24.
7. Adebajo MO, Frost RL, Kloprogge JT, Carmody O, Kokot S: **Porous Materials for Oil Spill Cleanup : A Review of Synthesis.** *J Porous Mater* 2003, **10**:159–170.
8. Choi HM, Cloud RM: **Natural sorbents in oil spill cleanup.** *Environ Sci Technol* 1992, **26**:772–776.

9. Ceylan D, Dogu S, Karacik B, Yakan SD, Okay OS, Okay O: **Evaluation of butyl rubber as sorbent material for the removal of oil and polycyclic aromatic hydrocarbons from seawater.** *Environ Sci Technol* 2009, **43**:3846–3852.
10. Mesquita SR, van Drooge BL, Reche C, Guimaraes L, Grimalt JO, Barata C, Pina B: **Toxic assessment of urban atmospheric particle-bound PAHs: relevance of composition and particle size in Barcelona (Spain).** *Environ Pollut* 2014, **184**:555–562.
11. Teas C, Kalligeros S, Zankos F, Stournas S, Lois E, Anastopoulos G: **Investigation of the effectiveness of absorbent materials in oil spills clean up.** *Desalination* 2001, **140**:259–264.
12. Zhu H, Qiu S, Jiang W, Wu D, Zhang C: **Evaluation of electrospun polyvinyl chloride/polystyrene fibers as sorbent materials for oil spill cleanup.** *Environ Sci Technol* 2011, **45**:4527–4531.
13. Deschamps G, Caruel H, Borredon ME, Bonnin C, Vignoles C: **Oil removal from water by selective sorption on hydrophobic cotton fibers. 1. Study of sorption properties and comparison with other cotton fiber-based sorbents.** *Environ Sci Technol* 2003, **37**:1013–1015.
14. Lin JY, Shang YW, Ding B, Yang JM, Yu JY, Al-Deyab SS: **Nanoporous polystyrene fibers for oil spill cleanup.** *Mar Pollut Bull* 2012, **64**:347–352.
15. Wu J, Wang N, Wang L, Dong H, Zhao Y, Jiang L: **Electrospun Porous Structure Fibrous Film with High Oil Adsorption Capacity.** *ACS Appl Mater Interfaces* 2012, **4**:3207–3212.

16. Lin J, Tian F, Shang Y, Wang F, Ding B, Yu J, Guo Z: **Co-axial electrospun polystyrene/polyurethane fibres for oil collection from water surface.** *Nanoscale* 2013, **5**:2745–55.
17. Lin J, Tian F, Shang Y, Wang F, Ding B, Yu J: **Facile control of intra-fiber porosity and inter-fiber voids in electrospun fibers for selective adsorption.** *Nanoscale* 2012, **4**:5316–5320.
18. Bianco A, Calderone M, Cacciotti I: **Electrospun PHBV/PEO co-solution blends: Microstructure, thermal and mechanical properties.** *Mater Sci Eng C-Materials Biol Appl* 2013, **33**:1067–1077.
19. Bognitzki M, Frese T, Steinhart M, Greiner A, Wendorff JH, Schaper A, Hellwig M: **Preparation of fibers with nanoscaled morphologies: Electrospinning of polymer blends.** *Polym Eng Sci* 2001, **41**:982–989.
20. Li D, Xia YN: **Electrospinning of nanofibers: Reinventing the wheel?** *Adv Mater* 2004, **16**:1151–1170.
21. Steyaert I, Van Der Schueren L, Rahier H, De Clerck K: **An alternative solvent system for blend electrospinning of polycaprolactone/chitosan nanofibres.** In *Macromolecular Symposia*; 2012.
22. Young TJ, Monclus MA, Burnett TL, Broughton WR, Ogin SL, Smith PA: **The use of the PeakForce™ quantitative nanomechanical mapping AFM-based method for high-resolution Young's modulus measurement of polymers.** *Meas Sci Technol* 2011, **22**.
23. Avila AF, Munhoz VC, De Oliveira AM, Santos MCG, Lacerda GRBS, Gonçalves CP:

Nano-based systems for oil spills control and cleanup. *J Hazard Mater* 2014, **272**:20–27.

24. Megelski S, Stephens JS, Chase DB, Rabolt JF: **Micro- and nanostructured surface morphology on electrospun polymer fibers.** *Macromolecules* 2002, **35**:8456–8466.

25. Lin JY, Ding B, Yu JY, Hsieh Y: **Direct Fabrication of Highly Nanoporous Polystyrene Fibers via Electrospinning.** *ACS Appl Mater Interfaces* 2010, **2**:521–528.

26. Ramakrishna K., Teo, W., Lim, T., Ma, Z. SF: *An Introduction to Electrospinning and Nanofibres.* 2005.

27. Wang LF, Pai CL, Boyce MC, Rutledge GC: **Wrinkled surface topographies of electrospun polymer fibers.** *Appl Phys Lett* 2009, **94**.

28. Casper CL, Stephens JS, Tassi NG, Chase DB, Rabolt JF: **Controlling surface morphology of electrospun polystyrene fibers: Effect of humidity and molecular weight in the electrospinning process.** *Macromolecules* 2004, **37**:573–578.

29. Wang N, Burugapalli K, Song W, Halls J, Moussy F, Zheng Y, Ma Y, Wu Z, Li K: **Tailored fibro-porous structure of electrospun polyurethane membranes, their size-dependent properties and trans-membrane glucose diffusion.** *J Memb Sci* 2013, **427**:207–217.

30. Jarusuwannapoom T, Hongrojjanawiwat W, Jitjaicham S, Wannatong L, Nithitanakul M, Pattamaprom C, Koombhongse P, Rangkupan R, Supaphol P: **Effect of solvents on electrospinnability of polystyrene solutions and morphological appearance of resulting electrospun polystyrene fibers.** *Eur Polym J* 2005, **41**:409–421.

31. Gao NW, Ke W, Fan YQ, Xu NP: **Evaluation of the oleophilicity of different alkoxysilane modified ceramic membranes through wetting dynamic measurements.** *Appl Surf Sci* 2013, **283**:863–870.
32. Cassie ABD, Baxter S: **Wettability of porous surfaces.** *Trans Faraday Soc* 1944.
33. Zhang H, Zhen Q, Cui JQ, Liu RT, Zhang YF, Qian XM, Liu Y: **Groove-shaped polypropylene/polyester micro/nanofibrous nonwoven with enhanced oil wetting capability for high oil/water separation.** *Polymer (Guildf)* 2020.
34. Sas I, Gorga RE, Joines JA, Thoney KA: **Literature review on superhydrophobic self-cleaning surfaces produced by electrospinning.** *J Polym Sci Part B-Polymer Phys* 2012, **50**:824–845.
35. Uyar T, Havelund R, Hacaloglu J, Zhou XF, Besenbacher F, Kingshott P: **The formation and characterization of cyclodextrin functionalized polystyrene nanofibers produced by electrospinning.** *Nanotechnology* 2009, **20**.
36. Huang C, Niu HT, Wu JL, Ke QF, Mo XM, Lin T: **Needleless Electrospinning of Polystyrene Fibers with an Oriented Surface Line Texture.** *J Nanomater* 2012.
37. Tanzi MC, Mantovani D, Petrini P, Guidoin R, Laroche G: **Chemical stability of polyether urethanes versus polycarbonate urethanes.** *J Biomed Mater Res* 1997, **36**:550–559.
38. Miller JA, Lin SB, Hwang KKS, Wu KS, Gibson PE, Cooper SL: **Properties of Polyether Polyurethane Block Copolymers - Effects of Hard Segment Length Distribution.** *Macromolecules* 1985, **18**:32–44.

39. Bahrami A, Bailly C, Nysten B: **Spatial resolution and property contrast in local mechanical mapping of polymer blends using AFM dynamic force spectroscopy.** *Polymer (Guildf)* 2019, **165**(September 2018):180–190.
40. Banerjee SS, Janke A, Gohs U, Heinrich G: **Electron-induced reactive processing of polyamide 6/polypropylene blends: Morphology and properties.** *Eur Polym J* 2018, **98**(September 2017):295–301.
41. Galuska AA, Poulter RR, McElrath KO: **Force modulation AFM of elastomer blends: Morphology, fillers and cross-linking.** *Surf Interface Anal* 1997, **25**:418–429.
42. Mrad O, Saunier J, Chodur CA, Rosilio V, Agnely F, Aubert P, Vigneron J, Etcheberry A, Yagoubi N: **A comparison of plasma and electron beam-sterilization of PU catheters.** *Radiat Phys Chem* 2010, **79**:93–103.
43. Mohamed A, Gordon SH, Biresaw G: **Poly(lactic acid)/polystyrene bioblends characterized by thermogravimetric analysis, differential scanning calorimetry, and photoacoustic infrared spectroscopy.** *J Appl Polym Sci* 2007, **106**:1689–1696.
44. Wagner A, Poursorkhabi V, Mohanty AK, Misra M: **Analysis of Porous Electrospun Fibers from Poly(L-lactic acid)/Poly(3-hydroxybutyrate-co-3-hydroxyvalerate) Blends.** *Acs Sustain Chem Eng* 2014, **2**:1976–1982.
45. Brostow W, Chiu R, Kalogeras IM, Vassilikou-Dova A: **Prediction of glass transition temperatures: Binary blends and copolymers.** *Mater Lett* 2008, **62**:3152–3155.
46. Teng D, Wahid A, Zeng Y: **Zein/PVDF micro/nanofibers with improved mechanical property for oil adsorption.** *Polymer (Guildf)* 2020.

47. Lee KH, Kim HY, Ryu YJ, Kim KW, Choi SW: **Mechanical behavior of electrospun fiber mats of poly(vinyl chloride)/polyurethane polyblends.** *J Polym Sci Part B-Polymer Phys* 2003, **41**:1256–1262.
48. Lou L, Kendall RJ, Smith E, Ramkumar SS: **Functional PVDF/rGO/TiO₂ nanofiber webs for the removal of oil from water.** *Polymer (Guildf)* 2020.
49. Arinstein A, Burman M, Gendelman O, Zussman E: **Effect of supramolecular structure on polymer nanofibre elasticity.** *Nat Nanotechnol* 2007.

Highlights

- Bi-component structure of PS and PU polymer blend was successfully electrospun.
- Fibre structure was dependent upon the blend ratio, solvent type and applied voltage
- DSC analysis shows strong miscibility existed between the two polymers (PS and PU)
- PU addition into the polymer matrix caused a significant boost in tensile strength
- Sorption capacity was 2-5 times higher than previous reports with other methods

Declaration of interests

The authors declare that they have no known competing financial interests or personal relationships that could have appeared to influence the work reported in this paper.

The authors declare the following financial interests/personal relationships which may be considered as potential competing interests:

Journal Pre-proof